PHYSICAL REVIEW D **89,** 063511 (2014)

Asymmetric sky from the long mode modulations

Ali Akbar Abolhasani,[1*] Shant Baghram,[2†] Hassan Firouzjahi,[2‡] and Mohammad Hossein Namjoo[1§]

[1]*School of Physics, Institute for Research in Fundamental Sciences (IPM), P. O. Box 19395-5531, Tehran, Iran*

[2]*School of Astronomy, Institute for Research in Fundamental Sciences (IPM), P. O. Box 19395-5531, Tehran, Iran*

(Received 11 December 2013; published 6 March 2014)

The observed hemispherical power asymmetry in cosmic microwave background radiation may have originated from the modulations of superhorizon long-wavelength modes. In this work, we unveil different aspects of asymmetries generated from the long-wavelength mode modulations. We show that the same mechanism that leads to the observed cosmic microwave background hemispherical power asymmetry via superhorizon long-mode perturbation also yields dipole asymmetry in (a) the tensor perturbations power spectrum and (b) the halo bias parameter. These are different phenomena relevant to different cosmological histories, but both share the same underlying mechanism in generating asymmetries in the sky. We obtain the set of consistency conditions relating the amplitude of dipole asymmetries generated on tensor perturbations and halo bias parameter to the amplitude of dipole asymmetry generated on cosmic microwave background power spectrum. In addition, we show that this mechanism does not produce dipole asymmetry in acceleration expansion in an ΛCDM Universe because the superhorizon curvature perturbation is conserved in this background.

DOI: 10.1103/PhysRevD.89.063511 PACS numbers: 98.80.Cq

I. INTRODUCTION

In theories of the early Universe, it is conceivable that our observable Universe is a patch of a much larger universe. For example, the inflationary period [1] does not necessarily last only 60 e-folds or so to solve minimally the horizon and the flatness problems today. But it is natural to imagine that inflation lasts longer. Indeed, we can think about preinflationary effects on our observable Universe. Two main preinflationary effects are bubble collisions and long-mode modulations. Historically, Grishchuk and Zeldovich were the first who proposed that the superhorizon perturbations can generate large-scale temperature fluctuations on the cosmic microwave background (CMB) [2].

The idea of looking for the fingerprints of the preinflationary physics in the sky is boosted again with the detection of hemispherical asymmetry on the CMB as reported by the Planck collaboration [3], which was also observed by Wilkinson Microwave Anisotropy Probe (WMAP) data [4]. In the case that the observed anomaly is not a statistical artifact, it can be viewed as a new challenge for simple single-field inflationary models [5,6]. In this venue, Erickcek *et al*. [7] and Gordon [8] argued that the modulation of the superhorizon perturbations can be the source of this asymmetry. However, this modulations must be treated carefully, since it can produce large temperature perturbations on the CMB map on which there are strict constrains on the departure from isotropy (mainly from quadrupole and octupole moments) [9].

The aim of this paper is not to study the fundamental origin of this long-mode modulation. Instead, assuming the existence of this large-amplitude long-wavelength mode, we would like to examine the consequences of such long-mode modulations on various cosmological parameters. In particular, we examine whether or not the same mechanism that generates dipolar asymmetry on the CMB power spectrum can also generate dipole asymmetry on (a) tensor perturbations, (b) the halo bias parameter, and (c) the dark energy acceleration expansion. Our findings show that the long modulation induces dipole asymmetry, at least, in principle, in cases (a) and (b) but not in case (c) in a ΛCDM background. We also relate the amplitude of dipole asymmetry generated in tensor perturbations and halo bias parameters to the amplitude of dipole asymmetry generated on the CMB power spectrum. In this view, our study provides a set of consistency conditions for the asymmetries generated on seemingly different cosmological observables and histories that can be tested in future observations; see also Ref. [5] for similar lines of thought. Having said this, recently, the possibility of exciting long-mode perturbations in open inflation models via bubble nucleation was put forward in Ref. [10], which is very intriguing.

A phenomenological parametrizations of the dipolar asymmetry is defined via

$$\mathcal{P}_{\mathcal{R}}^{1/2}(k,\mathbf{x}) = \mathcal{P}_{\mathcal{R}}^{1/2^{\rm iso}}(k)(1+A(k)\hat{\mathbf{p}}.\mathbf{x}/x_{\rm CMB}), \qquad (1)$$

*abolhasani@ipm.ir
†baghram@ipm.ir
‡firouz@mail.ipm.ir
§mh.namjoo@ipm.ir

in which $\mathcal{R}$ is the comoving curvature perturbation, $\mathcal{P}_{\mathcal{R}}(k,\mathbf{x})$ is the asymmetric curvature perturbations power spectrum, $\mathcal{P}^{\rm iso}_{\mathcal{R}}$ is the isotropic power spectrum, $A(k)$ is the amplitude of the dipolar asymmetry, the direction of anisotropy is shown by $\hat{\mathbf{p}}$, and $x_{\rm CMB}$ is the comoving distance to the surface of last scattering. The recent data from the Planck mission indicates that the amplitude of the asymmetry is $A = 0.072 \pm 0.022$ for large angular scales, $\ell < 64$. Data analysis shows that the best fit for the anisotropy direction is $(l,b) = (227,-27)$ [3].

As mentioned above, besides the observational effects on the CMB temperature fluctuations, the superhorizon long mode will also introduce nontrivial effects on the early and late-time cosmological observables. In Sec. II, we formulate the asymmetry induced from long-mode perturbations for general field fluctuations and apply this formalism for asymmetry generated in tensor perturbations. In Sec. III, we focus on the modulation of the halo bias parameter, and in Sec. IV, we study the effect of long modes on the deceleration parameter followed by discussions and conclusions in Sec. V. We present the technical analysis of calculating the cross-correlation between one scalar and two graviton perturbations in nonattractor backgrounds in the Appendix.

II. ASYMMETRY ON A GENERAL FIELD FLUCTUATION BY LARGE-SCALE PERTURBATION

In this section, we investigate how a long-wavelength scalar perturbation can modulate the statistics of a general field $\mathcal{O}$ on smaller CMB scales, yielding a hemispherical asymmetry on its power spectrum $\mathcal{P}_{\mathcal{O}}$. The field of interest, $\mathcal{O}$, is kept arbitrary, but we are mainly interested in the cases in which $\mathcal{O}$ represents the curvature perturbations $\mathcal{R}$ or the tensor perturbations. In particular, it is shown in Ref. [12] that when $\mathcal{O} = \mathcal{R}$ the amplitude of the dipole asymmetry in the curvature perturbation power spectrum, $A_{\mathcal{R}}$, is proportional to the amplitude of local non-Gaussianity, $f^{\rm loc}_{\rm NL}$. In deriving this conclusion, it was essential that only one field sources the curvature perturbation.

With this discussion in mind, now we extend the analysis in Ref. [12] for general $\mathcal{O}$. Similar to the single source assumption employed in Ref. [12], in what follows, we assume that only one field, say $\delta\phi$, has a non-negligible three-point cross correlation with $\mathcal{O}$, $\langle\delta\phi\mathcal{O}\mathcal{O}\rangle \neq 0$. That is, any other large-scale field, $\delta\sigma_i$, $i = 1, 2...$, has a negligible correlation in the form of $\langle\delta\sigma_i OO\rangle$, yielding negligible modulations[1]. Under the above assumptions, and as long as the above correlation is concerned, the long-wavelength mode is effectively the comoving curvature perturbation $\mathcal{R}_L$. In other words, the information in three-point function $\langle\delta\phi\mathcal{O}\mathcal{O}\rangle$ is encoded in $\langle\mathcal{R}\mathcal{O}\mathcal{O}\rangle$. This can be seen if one writes down $\mathcal{R}$ in terms of $\delta\phi$ and $\delta\sigma_i$ perturbations, $\mathcal{R} = c_\phi\delta\phi + \sum_i c_i\delta\sigma_i$, with some coefficients c_ϕ and c_i.

We are interested in asymmetry generated on the power spectrum of the operator $\mathcal{O}$ defined in Fourier space via

$$\langle\mathcal{O}_{\mathbf{k}}\mathcal{O}_{\mathbf{k}'}\rangle = (2\pi)^3\delta^3(\mathbf{k}+\mathbf{k}')P_{\mathcal{O}}(k), \qquad \mathcal{P}_{\mathcal{O}} \equiv \frac{k^3}{2\pi^2}P_{\mathcal{O}}(k). \tag{2}$$

Following the parametrizations given in Eq. (1), the dipole asymmetry in the power spectrum of $\mathcal{O}$ in Fourier space can be modeled by

$$\mathcal{P}_{\mathcal{O}}(k) \simeq \mathcal{P}^{\rm iso}_{\mathcal{O}}(k)(1 + 2A_{\mathcal{O}}(k)\hat{\mathbf{p}}.\mathbf{x}/x_n), \tag{3}$$

where $\mathcal{P}^{\rm iso}_{\mathcal{O}}(k)$ is the isotropic part of the power spectrum and $A_{\mathcal{O}}(k)$ represents the amplitude of the dipole asymmetry that we are interested in. By the above parametrizations, we can write

$$\frac{\nabla P_{\mathcal{O}_k}}{P_{\mathcal{O}_k}} \simeq \frac{2A_{\mathcal{O}}\hat{\mathbf{p}}}{x_n}, \tag{4}$$

which will be used later.

We assume that there exists a large superhorizon mode $\mathcal{R}_L$ with the amplitude $\mathcal{P}_{RL}$ and the comoving wave number k_L, superimposed on the entire observable Universe:

$$\mathcal{R}_L = \mathcal{R}_{k_L}\sin(\mathbf{k}_L.\mathbf{x}) = \mathcal{P}_{\mathcal{R}L}^{1/2}\sin(\mathbf{k}_L.\mathbf{x}). \tag{5}$$

Note that $\mathcal{P}_{\mathcal{R}L}$ is the power spectrum of the long mode obtained via ensemble averaging in a very large box [11]. In this view, for small-scale perturbations inside this very large box, $k \gg k_L$, the quantum fluctuations of $\mathcal{O}$ are treated as random statistical variables. In this view, the size of our observed Universe is given by H_0^{-1}, in which H_0 is the current Hubble constant but the long mode that causes the modulation has the wavelength $\lambda_L \gg H_0^{-1}$. As usual, for our small CMB-scale modes k, we work in the Fourier space with the volume V. For this picture to work, the volume of the Fourier space should be bigger than H_0^{-1} but smaller than λ_L, so we have the following hierarchy in mind:

$$H_0^{-3} < V \ll k_L^{-3}. \tag{6}$$

Now, let us parametrize the three-point cross correlation function $\langle\mathcal{R}(\mathbf{k}_L)\mathcal{O}(\mathbf{k}_1)\mathcal{O}(\mathbf{k}_2)\rangle$ in the squeezed limit $k_L \to 0$ by

$$\langle\mathcal{R}(\mathbf{k}_L)\mathcal{O}(\mathbf{k}_1)\mathcal{O}(\mathbf{k}_2)\rangle \equiv (2\pi)^3\delta(\mathbf{k_L}+\mathbf{k}_1+\mathbf{k}_2)\left(\frac{12}{5}f^{\mathcal{R}\mathcal{O}}_{\rm NL}\right)P_{\mathcal{R}}(k_L)P_{\mathcal{O}}(k_1). \tag{7}$$

[1]Actually, we need the weaker requirement that $\langle\delta\sigma_i OO\rangle \to 0$ in the squeezed limit $k_L \to 0$.

In this view, the parameter $f_{\rm NL}^{\mathcal{RO}}$ measures the three-point cross correlations of $\mathcal{R}$ and $\mathcal{O}$, which is a generalization of the usual local non-Gaussianity parameter $f_{\rm NL}^{\rm loc}$. Note that for $\mathcal{O}=\mathcal{R}$, we have $f_{\rm NL}^{\mathcal{RR}}=f_{\rm NL}^{\rm loc}$.

The essential point to note is that the effect of the long wavelength curvature perturbation on small-scale perturbations is just a rescaling of their background. This is because the small CMB-scale perturbations cannot probe the spatial variation associated with the long-wavelength perturbations $\mathbf{k}_L$. Consequently, we expect that the cosmological observations, which only probe the cosmic background will not be affected by long mode modulation. Keeping in mind that the curvature perturbation is not necessarily constant on superhorizon scales, this yields [12]

$$\langle\mathcal{R}(\mathbf{k_L})\mathcal{O}(\mathbf{k_1})\mathcal{O}(\mathbf{k_2})\rangle \simeq \langle\mathcal{R}(\mathbf{k_L})\langle\mathcal{O}(\mathbf{k_1})\mathcal{O}(\mathbf{k_2})\rangle_{\mathcal{R}(\mathbf{k_L})}\rangle$$
$$\simeq \left\langle\mathcal{R}(\mathbf{k_L})\left(\mathcal{R}(\mathbf{k}_L)\frac{\partial}{\partial\mathcal{R}(\mathbf{k_L})}\langle\mathcal{O}(\mathbf{k_1})\mathcal{O}(\mathbf{k_2})\rangle+\dot{\mathcal{R}}(\mathbf{k_L})\frac{\partial}{\partial\dot{\mathcal{R}}(\mathbf{k_L})}\langle\mathcal{O}(\mathbf{k_1})\mathcal{O}(\mathbf{k_2})\rangle\right)\right\rangle. \quad (8)$$

Here, $\langle\mathcal{O}(\mathbf{k_1})\mathcal{O}(\mathbf{k_2})\rangle_{\mathcal{R}(\mathbf{k_L})}$ means that we calculate $\langle\mathcal{O}(\mathbf{k_1})\mathcal{O}(\mathbf{k_2})\rangle$ in the background of $\mathcal{R}(\mathbf{k_L})$. To obtain the above relation, we have assumed the Bunch–Davies initial condition so the non-Gaussianity effects deep inside the horizon are negligible. Furthermore, as emphasized at the beginning of this section, it is essential that only one field has a nonzero three-point correlation with $\mathcal{O}$ so $\langle\mathcal{O}(\mathbf{k_1})\mathcal{O}(\mathbf{k_2})\rangle$ depends on the modulations of a single field that can be absorbed in $\mathcal{R}(k_L)$, as we did in Eq. (8).

Now comparing Eq. (7) with Eq. (8), one has

$$\frac{12}{5}f_{\rm NL}^{\mathcal{RO}}P_{\mathcal{R}_L}P_{\mathcal{O}}\simeq P_{\mathcal{R}_L}\frac{\partial P_{\mathcal{O}}}{\partial\mathcal{R}_L}+\frac{1}{2}\partial_t P_{\mathcal{R}_L}\frac{\partial P_{\mathcal{O}}}{\partial\dot{\mathcal{R}}_L}. \quad (9)$$

On the other hand, if $\mathcal{R}_L$ is responsible for the asymmetry of the power spectrum of field $\mathcal{O}$, we have

$$\nabla P_{\mathcal{O}}=\frac{\partial P_{\mathcal{O}}}{\partial\mathcal{R}_L}\nabla\mathcal{R}_L+\frac{\partial P_{\mathcal{O}}}{\partial\dot{\mathcal{R}}_L}\nabla\dot{\mathcal{R}}_L. \quad (10)$$

Noting that, in coordinate space, $\nabla\mathcal{R}_L=k_L\mathcal{R}_L$ and $\mathcal{R}_L=\mathcal{P}_{\mathcal{R}_L}^{1/2}$, we have

$$\mathcal{R}_L\nabla P_{\mathcal{O}}=\frac{\partial P_{\mathcal{O}}}{\partial\mathcal{R}_L}k_L\mathcal{P}_{\mathcal{R}_L}+\frac{1}{2}\frac{\partial P_{\mathcal{O}}}{\partial\dot{\mathcal{R}}_L}k_L\dot{\mathcal{P}}_{\mathcal{R}_L}. \quad (11)$$

Comparing this with Eq. (9) yields

$$\frac{\nabla P_{\mathcal{O}}}{P_{\mathcal{O}}}\simeq\frac{12}{5}f_{\rm NL}^{\mathcal{RO}}\mathbf{k}_L\mathcal{P}_{\mathcal{R}_L}^{1/2}. \quad (12)$$

Finally, using Eq. (4), one obtains

$$A_{\mathcal{O}}\simeq\frac{6}{5}f_{\rm NL}^{\mathcal{RO}}x_nk_L\mathcal{P}_{\mathcal{R}_L}^{1/2}. \quad (13)$$

This is one of the main results for this section. This formula relates $A_{\mathcal{O}}$, the amplitude of the dipole asymmetry in $P_{\mathcal{O}}$, to the cross-term coupling $f_{\rm NL}^{\mathcal{RO}}$ and the amplitude of the long-mode perturbations $\mathcal{P}_{\mathcal{R}_L}^{1/2}$.

Now, we can use Eq. (13) to obtain the amplitude of modulation for some interesting examples.

A. CMB power spectrum dipole asymmetry

The first example corresponds to the case $\mathcal{O}=\mathcal{R}$, so we can calculate the dipole asymmetry in the CMB power spectrum similar to Refs. [12–18]; see also Refs. [19–21]. With $f_{\rm NL}^{\mathcal{RR}}=f_{\rm NL}^{\rm loc}$, the amplitude of the CMB dipole asymmetry, $A_{\mathcal{R}}$, from Eq. (13) is obtained to be

$$A_{\mathcal{R}}\simeq\frac{6}{5}f_{\rm NL}^{\rm loc}x_nk_L\mathcal{P}_{\mathcal{R}_L}^{1/2}. \quad (14)$$

To obtain observable dipolar asymmetry from the long-mode modulation, one needs $\mathcal{P}_{\mathcal{R}_L}\gg\mathcal{P}_{\mathcal{R}}(k_{\rm CMB})$. However, for perturbations to be under control, we require $\mathcal{R}_L^2\simeq\mathcal{P}_{\mathcal{R}_L}(k_L)\lesssim 1$. On the other hand, imposing the octupole Q_3 constraints on CMB anisotropies [9,12] yields

$$\frac{6}{5}(k_Lx_n)\mathcal{P}_{\mathcal{R}_L}^{1/2}\lesssim 32Q_3{}^{1/3}\sim 10^{-1}. \quad (15)$$

Plugging Eq. (15) in Eq. (14), we obtain our upper bound consistency condition for the amplitude of the CMB dipolar asymmetry [12]

$$|A_{\mathcal{R}}|\lesssim 10^{-1}|f_{\rm NL}^{\rm loc}|. \quad (16)$$

However, it is pointed out in Refs. [9,13] that there is another term in the total curvature perturbation proportional to $\mathcal{R}_L^2$. This brings another constraint from the quadrupole Q_2 on CMB. This changes the above bound to [9,13]

$$|A_{\mathcal{R}}|\lesssim 0.02|f_{\rm NL}^{\rm loc}|^{1/2}. \quad (17)$$

See, however, Ref. [22] for a possible way to avoid this bound. To obtain observable dipole asymmetry consistent with the Planck observation, we need $|A_{\mathcal{R}}|=0.07\pm0.02$.

Equation (17) is an interesting result, relating the amplitude of the hemispherical asymmetry to the level

of non-Gaussianity in the system. This was first obtained by Lyth in Ref. [13] for the conventional curvaton scenario in which the entire curvature perturbation is sourced by the curvaton field. For the single-field attractor models of inflation with the Bunch–Davies initial condition in which the level of non-Gaussianity is related to the spectral index n_s via [23] $f_{\rm NL}^{\rm loc} \sim n_s - 1$, Eq. (17) yields $|A_{\mathcal{R}}| \lesssim 10^{-2}(n_s-1)^{1/2} \sim 10^{-3}$, which is too small to be observable.

As speculated in Ref. [12], one can obtain large hemispherical asymmetry in models of nonattractor single-field inflation in which the curvature perturbation is not frozen on a superhorizon scale and large observable non-Gaussianity can be generated independent of n_s via [24–27]

$$f_{\rm NL}^{\rm loc} = \frac{5(1+c_s^2)}{4c_s^2}, \tag{18}$$

where c_s is the sound speed of cosmological perturbations during the nonattractor phase. With $f_{\rm NL}^{\rm loc} \sim$ few, one can saturate both the Planck constraints on local non-Gaussianity [28] and the observed CMB bipolar asymmetry. As discussed in Ref. [12], Eq. (18) holds only during the short nonattractor phase, which precedes the last 60 or so e-folds of inflation. As a result, once the attractor phase of inflation has been reached, one obtains the usual relation $f_{\rm NL} \sim n_s - 1$, so the amplitude of bipolar asymmetry on smaller CMB scales rapidly becomes negligible. This built-in scale dependence of $f_{\rm NL}$ can address the quasar constraints on $A_{\mathcal{R}}$ on scales smaller than Mpc^{-1} [29].

B. Tensor perturbations asymmetry

As a second interesting example, we obtain the amplitude of the dipole asymmetry in the tensor perturbations power spectrum, A_T, induced by the long-wavelength mode.

Consider the three-dimensional spatial metric on the surface of constant time [23]

$$ds_{(3)}^2 = a(t)^2 e^{2\mathcal{R}(t,\mathbf{x})} {}^{(3)}g_{ij} d\mathbf{x}^i d\mathbf{x}^j, \tag{19}$$

in which

$${}^{(3)}g_{ij} = \delta_{ij} + h_{ij} + \frac{1}{2}h_{il}h_{lj} + \ldots, \qquad \partial_i h_{ij} = h_{ii} = 0. \tag{20}$$

With this convention, $\det {}^{(3)}g_{ij} = 1$ and h_{ij} represents the two degrees of freedom associated with the tensor perturbations.

Setting $\mathcal{O} = h_{ij}$ in Eq. (7) and parametrizing the cross-correlation function $\langle \mathcal{R} h_{ij} h_{kl} \rangle$ by $f_{\rm NL}^{\mathcal{R}h}$, the amplitude of the tensor perturbations dipole asymmetry, A_T, from Eq. (13), is obtained to be

$$A_T \simeq \frac{6}{5} f_{\rm NL}^{\mathcal{R}h} x_n k_L \mathcal{P}_{\mathcal{R}_L}^{1/2}. \tag{21}$$

This is an interesting result: if there is an enhanced large-scale curvature perturbation that modulates the CMB curvature perturbations, it can also modulate the tensor perturbations power spectrum. The amplitude of this enhancement is controlled by $f_{\rm NL}^{\mathcal{R}h}$, which measures the cross-correlation $\langle \mathcal{R} h_{ij} h_{kl} \rangle$. Comparing the amplitude of tensor modulation in Eq. (21) to the corresponding scalar perturbation modulation $A_{\mathcal{R}}$ given in Eq. (14), we obtain the following consistency condition:

$$\frac{A_T}{A_{\mathcal{R}}} \simeq \frac{f_{\rm NL}^{\mathcal{R}h}}{f_{\rm NL}^{\rm loc}}. \tag{22}$$

Note that the above relation is valid for all single-field inflationary models with the Bunch– Davies initial condition, including nonattractor models. It is worth it to mention that the tensor perturbations freeze out after horizon crossing independent of the model of inflation. As a result, any correlation and modulation for the tensor field occurs during inflation and mainly at the time of horizon crossing. However, depending on the model, the curvature perturbation can evolve even after inflation and still has a chance to have correlation with other fields. This is particularly the case in models of multiple-field inflation such as in a curvaton scenario in which the curvature perturbations are generated at or after the end of inflation by light fields other than the inflaton field. Hence, Eq. (22) does not work for, e.g., the curvaton model. In such models, the curvaton field does not contribute to the inflationary phase, either at the background level or to perturbations. As a result, the tensor perturbation can correlate only with the inflaton field at horizon crossing. However, after inflation, this is the curvaton field that has the main role in perturbations and modulating the curvature perturbation.

Let us consider the models of single-field slow-roll inflation. As mentioned before, we know that these models can not generate the observed CMB dipole asymmetry, i.e., for these models, $A_{\mathcal{R}} \ll 0.07$. However, we consider these models as a platform to demonstrate the implication of our consistency condition Eq. (22) as a proof of concept. From Maldacena's analysis [23], $f_{\rm NL}^{\rm loc}$ and $f_{\rm NL}^{\mathcal{R}h}$ are related to the curvature perturbations spectral index n_s and to the tensor perturbation spectral tilt n_T via

$$\frac{12}{5} f_{\rm NL}^{\rm loc} = -(1-n_s), \qquad \frac{12}{5} f_{\rm NL}^{\mathcal{R}h} = 2\epsilon = -n_T, \tag{23}$$

in which $\epsilon = -\dot{H}/H^2$ is the slow-roll parameter and H is the Hubble expansion rate. Also note that n_T is related to the ratio of the amplitude of the tensor perturbations to the amplitude of the scalar perturbations via the consistency condition $r = 16\epsilon = -8n_T$. As a result, Eq. (22) yields

$$\left|\frac{A_T}{A_{\mathcal{R}}}\right| \simeq \frac{n_T}{n_s - 1} = \frac{r}{8(1-n_s)}. \tag{24}$$

Observationally, this is a very interesting result in which the ratio of the dipole asymmetries in tensor perturbations and the scalar perturbations is given by the ratio of n_T and $1 - n_s$. This is a hybrid of the two consistency relations $f_{\rm NL}^{\rm loc} \sim 1 - n_s$ and $r = -8n_T$. As an estimation of A_T, using the Planck constraints $r \lesssim 0.13$ and $n_s \simeq 0.96$, from Eq. (24), we obtain $A_T \lesssim 0.4 A_{\mathcal{R}}$. With the observational bound $A_{\mathcal{R}} \simeq 0.07$, this yields the prediction $A_T \lesssim 0.03$. It is interesting to see whether or not the upcoming analysis of the CMB polarization data by the Planck team can detect this level of hemispherical asymmetry on tensor perturbations.

As mentioned above, Eq. (24) holds for the single-field attractor models with the initial Bunch–Davies vacuum in which the Maldacena's consistency relations, Eq. (23), are at work. However, as mentioned above, simple single-field models of inflation cannot produce large enough dipole asymmetry, i.e., $A_{\mathcal{R}} \ll 0.07$ in these scenarios. Therefore, single-field slow-roll models predict $A_T \ll 0.03$. This is too small to be detected observationally. Therefore, one has to look for alternatives.

As shown in Ref. [12] and in the previous subsection, the single-field nonattractor models that violate Maldacena's consistency condition are able to produce a large observable dipole asymmetry as given in Eq. (18). Therefore, it is an interesting question to calculate the correlation function $\langle \mathcal{R}h^2 \rangle$ directly in nonattractor models to obtain $f_{\rm NL}^{\mathcal{R}h}$. This analyses were performed in the Appendix A. The shape of the bispectrum as given in Eq. (A7) is very different than the results obtained by Maldacena. There are two reasons for this. First, since $\mathcal{R}$ evolves on superhorizon scales, the profile of its wave function is different than that of the usual attractor model. This has to be taken into account when calculating the in-in integrals. Second, in the process of field redefinition (see the Appendix for details), unlike in Maldacena's analysis, one cannot neglect terms containing $\dot{\mathcal{R}}$. However, in the squeezed limit in which $k_L \ll k_1 \simeq k_2$, the shape function in Eq. (A7) collapses to the result obtained by Maldacena in the attractor phase as given in Eq. (A8). As a result, the relation $f_{\rm NL} \sim \epsilon$ as given in Eq. (23) still holds for nonattractor models. However, we note that the relation between $n_s - 1$ and $f_{\rm NL}^{\rm loc}$ as given in Eq. (23) does not hold in nonattractor model, and one has to use Eq. (18). Using the expressions for $f_{\rm NL}^{\mathcal{R}h}$ and $f_{\rm NL}^{\rm loc}$, respectively, from Eqs. (23) and (18), we obtain

$$\frac{A_T}{A_{\mathcal{R}}} \simeq \frac{2\epsilon c_s^2}{3(1+c_s^2)} = \frac{c_s r}{24(1+c_s^2)}, \tag{25}$$

in which, in the second equality, the relation $r = 16 c_s \epsilon$ has been used. This equation should be compared with Eq. (24) obtained for the attractor models.

In models of nonattractor inflation, ϵ decays like $\epsilon \propto a^{-6}$ [24], so at the end of nonattractor phase, ϵ and r become exponentially small (assuming the nonattractor phase has a few e-foldings). This means that the amplitudes of tensor perturbations are very small in the nonattractor model [25]. Therefore, the ratio A_T/A_R in the nonattractor phase is much smaller than the corresponding value in conventional slow-roll models. Taking $r \lesssim 0.1$ and $c_s \lesssim 1$, we obtain $A_T \simeq 3 \times 10^{-4}$. It is unlikely that the future cosmological observations can detect such a small dipole asymmetry in the tensor perturbations power spectrum.

To summarize, here, we have shown that the long-mode modulation induces dipole asymmetry not only on the curvature perturbations power spectrum but also on the tensor mode perturbations power spectrum. However, none of the single-field models studied so far can generate detectable dipole asymmetry on the tensor power spectrum. For the single-field slow-roll model, $A_T \ll 0.03$ because $A_{\mathcal{R}}$ generated in these models is too small to match the observed value. On the other hand, for the nonattractor models, A_T is even smaller than this value because, in these models, the amplitudes of tensor perturbations are suppressed. As a result, to obtain detectable dipole asymmetry in the tensor perturbations power spectrum, one has to look for multiple-field models in which more than one field contributes to the curvature perturbations. In multiple-field scenarios, the specific formulas Eqs. (24) and (25) do not hold. Therefore, for a given multiple-field inflation model, one has to explicitly calculate $\langle \mathcal{R}h^2 \rangle$ and correspondingly obtain the amplitude of $f_{\rm NL}^{\mathcal{R}h}$ and see whether large enough A_T is generated.

III. MODULATED BIAS

In this section, we show how the long-wavelength modulation $\mathcal{R}_L$ from curvature perturbation can affect the distribution of galaxies in sky through the halo bias parameter. The large-scale structure observables deal with the statistics of luminous matter, (i.e., galaxies and cluster of galaxies) sitting in the center of dark matter halos [30]. The statistics of galaxies such as the correlation functions, power spectrum, and the probability distribution function are related to the dark matter halo statistics. With the assumption that each dark matter halo is a host of a galaxy [31], this relation is parametrized through bias parameter $b = \delta_h/\delta_m$, where δ_h and δ_m are the halo density perturbation and the dark matter density perturbation, respectively. To show the effect of long-wavelength modulation, we study its effect on the threshold of nonlinear structure formation. In spherical collapse [32], a region of R undergoes a gravitational instability when its density perturbation becomes greater than the critical density $\delta_c \simeq 1.68$. This is obtained by considering the evolution of an overdense region in the cosmological background. The overdense region behaves like a closed Friedmann Universe with spatial curvature Δk and density of $\bar{\rho}_M + \Delta\rho_M$, where $\bar{\rho}_M$ is

the background density and $\Delta\rho_M$ is the excess density. The critical density $\delta_c = \Delta\rho_{M(c)}/\bar{\rho}_M$ is related to the critical excess of mass $\Delta\rho_{M(c)}$, where the structure enters the nonlinear regime.

In a recent work [33], it was shown that the bias parameter is a potential important observable in Large Scale Structure (LSS) to detect the primordial anisotropy through the nonlinear effect (non-Gaussianity). In this work, we just investigate the effects of anisotropy induced from the long-wavelength mode in the linear regime due to its effect on the critical density.

To study the effects of the long-mode modulation on the statistics of the structures, we use the peak-background splitting method [34], where the total matter density contrast $\delta \equiv \delta\rho_m/\rho_m$, is separated into the long and short wavelengths

$$\delta = \delta_s + \delta_l + \delta_L, \tag{26}$$

where δ_s is the density contrast of the structure associated with the short wavelength, δ_l is the density contrast from the long-wavelength mode in the observable Universe, and δ_L represents the density perturbation originating from $\mathcal{R}_L$. (The different scales presented in this splitting are shown in Fig. 1). The criteria to have a structure is that the local density perturbation δ_s of structure passes the critical density threshold, satisfying the condition

$$\delta_s > \delta_c^{\rm eff} \equiv \delta_c - \delta_l - \delta_L, \tag{27}$$

where we have assumed that the scale of structures is much smaller than the Hubble radius, $\lambda_s \ll H_0^{-1}$. Consequently, we assume that the effect of superhorizon long-mode modulation is similar to the effect of the long mode inside horizon. Both long modes change the critical density by the amount calculated in Eq. (27). Another important point to emphasize here is that we want to compare the statistics of structures in two different spatial positions where the amplitude of long-mode modulation is slightly different. This means that the mean density of matter is almost the same inside the Hubble radius, while the perturbations are slightly different in the dipole direction.

The long-wavelength mode changes the spherical collapse threshold, so we expect to have a change in the statistics of the structures in the Universe. We would like to calculate the probability of having structures with mass $M \equiv 4/3\pi R^3\rho_m$ (or equivalently the regions of radius R) and accordingly to calculate the bias parameter. To go further, we define the effective height parameter as

$$\nu_{\rm eff} \equiv \frac{\delta_c^{\rm eff}}{\sigma(M)} = \nu - \frac{\delta_l + \delta_L}{\sigma(M)}, \tag{28}$$

in which $\nu \equiv \delta_c/\sigma(M)$ and $\sigma(M)$ is the mass variance. The ν parameter plays a crucial role in the statistics of the collapsed object. In Fig. 2, we plot the height parameter vs the redshift. For high mass objects in the Universe, the variance is lower; consequently, the height parameter is larger (meaning that their statistics are smaller). The redshift dependence of the height parameter comes from the growth function of structures. As the Universe becomes dark-energy dominated, the growth of the structures decreases; consequently, we will have a small mass density

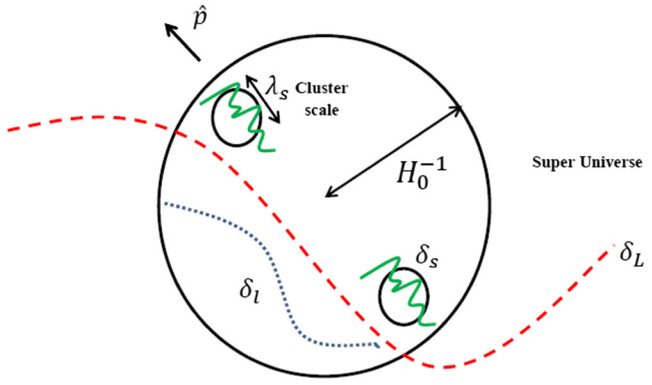

FIG. 1 (color online). This is a schematic figure representing perturbation scales in a peak-background splitting scenario. The large black-solid circle represents our observable Universe with radius H_0^{-1}, which is situated inside the super Universe. The small black-solid circles represent the structures (i.e., Galaxy clusters) in scale of Mpc. The green solid wavy curves represent the density contrasts in structure scale δ_s. The blue dotted curve is the long-mode perturbation δ_l inside the horizon. The red long-dashed curve is the superhorizon mode δ_L in the asymmetry direction $\hat{p}$.

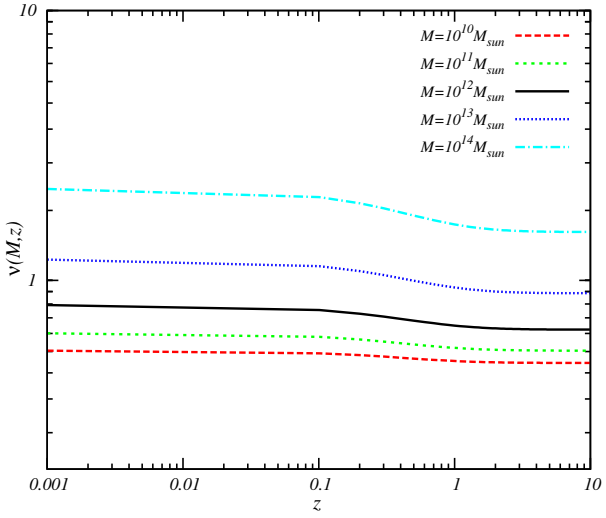

FIG. 2 (color online). In this figure, we plot the height parameter $\nu = \delta_c/\sigma(M,z)$ vs redshift for different mass scales that are probed via LSS. The black solid line indicates the height parameter for $M = 10^{12}M_\odot$, which is a typical mass scale of luminous red galaxies.

and larger height function. The shift in height parameters occurs in $z \sim 0.3$ as in Fig. 2.

Now, we can define the bias parameter from the modulated number density of the structures. The halo density contrast is defined as

$$\delta_h = \frac{n(M,\nu_{\rm eff}) - \bar{n}(M)}{\bar{n}(M)}, \tag{29}$$

where $\bar{n}(M)$ is the background number density of structures with mass M and $n(M,\nu_{\rm eff})$ is the modulated number density. Now, the bias parameter is defined as

$$b = -\frac{1}{\sigma(M)}\frac{\partial \ln \bar{n}(M)}{\partial \nu} = -\frac{1}{\sigma(M)}\frac{f'}{f}, \tag{30}$$

where we assumed the universality condition for the mass function of structures, which means that they are only a function of the height parameter, $\bar{n}(M) \propto f(\nu)$. The prime here and below indicates the derivative with respect to ν. Now, the bias parameter becomes a function of δ_L, in contrast to the standard case.

Considering the fact that both δ_l and δ_L should be smaller than the critical density and also $\delta_l \gg \delta_L$ so the effect of long mode modulation is subleading, we can expand the bias parameter in terms of δ_L as

$$b = b_0 + \frac{\partial b_0}{\partial \delta_L}\delta_L = b_0 - \frac{1}{\sigma(M)} b_0{}'\delta_L, \tag{31}$$

where b_0 represents the background unmodulated bias. Now, we can go further and write the bias parameter in the terms of universality function f and b_0 as

$$b(\mathbf{x}) = b_0 + b_0^2\left(\frac{f''f}{f'^2} - 1\right)\delta_L. \tag{32}$$

Correspondingly, the gradient of bias associated with the long-wavelength mode is obtained to be

$$\frac{\nabla b(\mathbf{x})}{b} = b_0\left(\frac{f''f}{f'^2} - 1\right)\nabla\delta_L \equiv b_0\mathcal{F}(\nu)\nabla\delta_L, \tag{33}$$

in which

$$\mathcal{F}(\nu) \equiv \frac{f''f}{f'^2} - 1. \tag{34}$$

To go further, we can relate the long-mode modulation of density perturbation to modulation in the Bardeen potential via the Poisson equation,

$$\delta_L = \frac{2}{3}\frac{\nabla^2\Phi}{(1+z)H_0^2\Omega_m^0} \simeq \frac{2}{5}\frac{D(z)\nabla^2\mathcal{R}_{L\,\rm pri}}{H_0^2\Omega_m^0} = \bar{M}(z)\bar{\nabla}^2\mathcal{R}_{L\,\rm pri}, \tag{35}$$

where $D(z)$ is the growth factor, Ω_m^0 is the current fraction of matter energy density, $\bar{M}(z) \equiv 2D(z)/5\Omega_m^0$, and $\bar{\nabla}^2 \equiv \nabla^2/H_0^2$. To obtain the approximate equality in Eq. (35), we assumed that for the very long wavelength the transfer function is unity, $T(k) \simeq 1$ (i.e., the growth of the potential function is scale independent). In this case, we use the relation $\Phi = \frac{9}{10}(1+z)D(z)\Phi_{\rm pri}$ in which $\Phi_{\rm pri}$ represents the primordial value of Φ at the start of radiation (end of reheating), which is related to the primordial value of R_L via $\Phi_{\rm pri} = \frac{2}{3}\mathcal{R}_{L\,\rm pri}$. Consequently, the gradient of the bias is obtained to be

$$\frac{\nabla b(x)}{b} \simeq b_0\mathcal{F}\bar{M}(z)\nabla(\bar{\nabla}^2\mathcal{R}_{L\,\rm pri}). \tag{36}$$

Interestingly we see that the gradient in bias is related to the gradient in $\nabla^2\mathcal{R}_{L\,\rm pri}$. This analysis also shows another manifestation of the long-wavelength mode's effect on cosmological parameters. It shows that, if the long-mode modulation is the source of dipole asymmetry on the CMB power spectrum, it will also induce dipole asymmetry on the LSS bias parameter. The long-mode modulation introduces the asymmetry in the bias parameter because of its effect on perturbations. As we have indicated in the introduction, the long-mode modulation does not affect the background because of the rescaling, but it shows up at the perturbation level.

Let us define the amplitude of the bias dipole asymmetry A_b via

$$b = b_0(1 + A_b\hat{\mathbf{x}}.\hat{\mathbf{p}}). \tag{37}$$

As a result, the gradient of the bias parameter is translated into

$$\frac{\nabla b}{b_0} = \frac{A_b\hat{\mathbf{p}}}{x_{\rm LSS}}, \tag{38}$$

where $x_{\rm LSS}$ is the comoving distance from the observer to the structure where the bias parameter is measured.

So far, our discussions were generic and model independent. Now, we assume that the long-mode modulation has the simple sinusoidal form as given in Eq. (5). Combining Eqs. (36) and (38), the anisotropy bias parameter can be written as

$$\begin{aligned} A_b &\simeq b_0\mathcal{F}(\nu)x_{\rm LSS}\bar{M}(z)\nabla(\bar{\nabla}^2\mathcal{R}_{L\,\rm pri}) \\ &= b_0\mathcal{F}(\nu)\bar{M}(z)\left(\frac{x_{\rm LSS}}{x_{\rm CMB}}\right)\left(\frac{k_L}{H_0}\right)^2[k_L x_{\rm CMB}\mathcal{P}_{\mathcal{R}_L}^{1/2}]. \end{aligned} \tag{39}$$

To simplify further, we assume the initial conditions are Gaussian and the probability function of structure formation has a universal form, $n(M) \propto f(\nu)$. To be more specific, we assume the Press– Schechter universality function [35], in which

$$f(\nu) = \frac{\nu}{\sqrt{2\pi}} e^{-\nu^2/2} \tag{40}$$

and

$$\mathcal{F}(\nu) = -\frac{\nu^2 + 1}{(\nu^2 - 1)^2}. \tag{41}$$

For almost all observational cases in which $\nu \ll 1$, $\mathcal{F}$ is a decreasing function of ν. Furthermore, $\mathcal{F}$ diverges at $\nu = 1$, corresponding to very high massive cluster of galaxies ($\mathcal{O} \sim 10^{14} M_\odot$). However, because of the low statistics of the cluster of galaxies, this is not suitable to obtain the bias parameter with the present and near-future cosmological data.

Now, we can use the observational constraint [12] $k_L x_{\rm CMB} \mathcal{P}^{1/2}_{\mathcal{R}_L} \leq 10^{-1}$ to put an upper bound on the bias parameter anisotropy. On the other hand, the detection of dipole anisotropy in CMB, $A \simeq 0.07$, and the assumption of non-Gaussianity at the order of $f_{\rm NL} \leq 10$ (which is compatible with Planck data) can be used to put an upper bound on the anisotropic bias as

$$0.007 \times b_0 \mathcal{F}(\nu) \bar{M}(z) \left(\frac{x_{\rm LSS}}{x_{\rm CMB}}\right) \left(\frac{k_L}{H_0}\right)^2 \leq A_b \leq 10^{-1} \times b_0 \mathcal{F}(\nu) \bar{M}(z) \left(\frac{x_{\rm LSS}}{x_{\rm CMB}}\right) \left(\frac{k_L}{H_0}\right)^2. \tag{42}$$

This is our main result in this section.

In a realistic case, taking the galaxy samples from Sloan Digital Sky Survey data release 9 [36], the mean redshift of the survey is set to $z = 0.57$, which results in $\bar{M} \sim 1$ and $x_{\rm LSS}/x_{\rm CMB} \sim 2200/14000 \sim 0.15$. Furthermore, the linear bias parameter obtained from the red luminous galaxies with $\nu \sim 0.8$ is $b_0 \sim 0.8$ and $|\mathcal{F}| \sim 12.5$. Taking the long mode to be, say, twice as big as the Hubble radius, $k_L/H_0 \sim 1/2$, the upper bound on the amplitude of the bias dipole is obtained to be

$$A_b(z \simeq 0.5) \leq 3 \times 10^{-2}. \tag{43}$$

We have omitted our lower bound on the asymmetric bias because the long-mode modulation could be much longer than the observable Universe and make the lower bound very small. This value is too small to be observed by today's large-scale surveys but will be observable with the future large-scale structure surveys like Large Synoptic Survey Telescope (LSST). Indeed, this is within the error bar of the bias parameter and the errors originated from the peculiar velocity. The LSST, which is designed to obtain a photometric redshift for 4 billion galaxies with the distribution peaking around $z = 1$, can be used to determine the galaxy bias with high accuracy. The galaxy cluster count with a combination of other cosmological observations, such as the weak gravitational lensing and CMB data, can measure the bias parameter in the redshift range between 0 to 1, with a precision as good as 2% accuracy [37]. Consequently, the anisotropy change in the bias parameter must be greater than this error bar (systematic and statistic errors) to be detected in this redshift range.

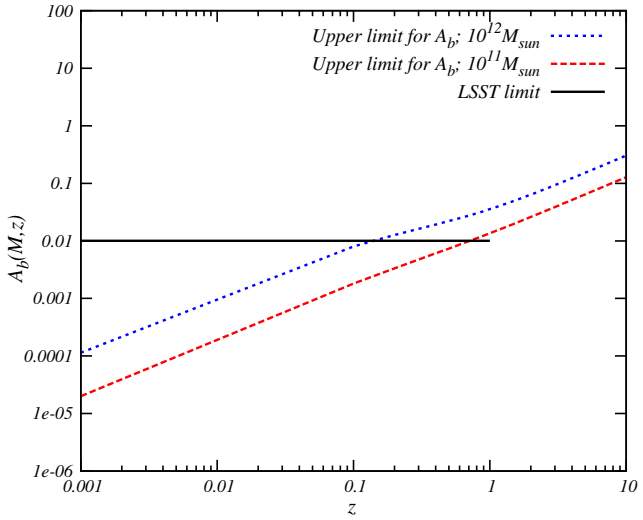

FIG. 3 (color online). In this figure, we have plotted the bias anisotropy upper bound vs redshift, assuming the universal mass function of Press–Schechter formalism. We have set $M = 10^{11} M_\odot$ (red long-dashed line) and $M = 10^{13} M_\odot$ (blue dashed line) and $k_L/H_0 = 1/2$. The solid black horizontal line indicates the upper limit precision of the LSST project.

In Fig. 3, we plotted the bias anisotropy parameter vs redshift for two different mass scales, in which we calculated the bias parameter. The figure shows that in an optimistic case with high redshift $z \sim 1$ the upper bound of the LSST is lower than the anisotropy calculated from a long mode with the size twice the size of the observable Universe. In a optimistic situation, if one can measure the matter power spectrum in 21 cm in future observations such as Square Kilometre Array with $z \sim 10$, which results in $\bar{M} \sim 1.5$ and $x_{\rm LSS}/x_{\rm CMB} \sim 10000/14000 \sim 0.7$ and assuming the same values for linear bias, $\mathcal{F}(\nu)$ and k_L/H_0, we obtain

$$A_b(z \simeq 10) \leq 2 \times 10^{-1}. \tag{44}$$

This is an $\mathcal{O}(20\%)$ change in the bias parameter. This is within the range of the observational detection.

IV. DIPOLE ASYMMETRY IN ACCELERATION EXPANSION?

Since we have studied dipole asymmetries generated in the tensor perturbations power spectrum and halo bias parameter, it is an interesting question if one searches for dipole asymmetries in late-time cosmological phenomena. In particular, we look into the possibility of generating dipole asymmetry in dark-energy acceleration expansion induced from the long-mode modulation. Somewhat

related to this idea, Kolb *et al*. [38] have employed the idea of superhorizon perturbations to explain the late-time cosmological acceleration. But shortly after their proposal, it was shown that this idea does not work [39,40].

Employing the separate universe approach, the line element in the comoving gauge in the presence of long-wavelength modulation is

$$ds^2 = -dt^2 + \bar{a}^2(t)e^{2\mathcal{R}_L(\mathbf{x},t)}\delta_{ij}dx^i dx^j, \tag{45}$$

in which $a(t)$ is the background (average) scale factor of our patch and $\mathcal{R}$ denotes the curvature perturbation in the comoving gauge. Again we do not mention the origin of this modulation or its shape, but we just assume that this modulation can have slight variations in our observable patch. What we have in mind is that this modulation is the same that caused the hemispherical asymmetries in the CMB power spectrum, in the tensor perturbations power spectrum, and in the bias that were studied in previous sections. In this view, all we need is that there exists a long-mode modulation with large amplitude, i.e., $\mathcal{P}_{\mathcal{R}_L} \gg \mathcal{P}_{\mathcal{R}_{\rm CMB}}$.

The above form of the metric suggests that the effective scale factor in each Hubble patch is given by

$$a(\mathbf{x},t) = \bar{a}(t)e^{\mathcal{R}(\mathbf{x},t)}. \tag{46}$$

As a result, the effective Hubble expansion rate, $H = \dot{a}/a$, is given by

$$H(\mathbf{x},t) = \bar{H}(t) + \dot{\mathcal{R}}_L(\mathbf{x},t), \tag{47}$$

in which $\bar{H}(t)$ represents the background homogeneous Hubble parameter. This equation suggests that the Hubble expansion rate is modified in the presence of the long-wavelength mode. It is important to note that if $\mathcal{R}_L$ is time independent, then it has no effect on H because, in this limit, $\mathcal{R}_L$ can be absorbed into a rescaling of $d\mathbf{x}^i$ without affecting the expansion dynamics. Naively, one may imagine that a mild variation of $\mathcal{R}_L$ across the observable patch may result in a variation in H. Here, we examine this idea critically for the case in which the acceleration expansion is driven by a cosmological constant to see whether or not $\mathcal{R}_L$ can be time dependent in a late-time accelerating universe.

It is convenient to work with the deceleration parameter q defined via

$$q \equiv -\frac{a\ddot{a}}{\dot{a}^2}. \tag{48}$$

With the effective scale factor and the Hubble parameter given in Eqs. (46) and (47), and to linear order in $\mathcal{R}_L \ll 1$ and $\dot{\mathcal{R}}/H \ll 1$, we get

$$q(\mathbf{x}) \simeq \bar{q} - \frac{2\dot{\mathcal{R}}_L(\mathbf{x})}{\bar{H}}(1+\bar{q}) - \frac{\ddot{\mathcal{R}}_L(\mathbf{x})}{\bar{H}^2}, \tag{49}$$

in which $\bar{q}$ represents the background homogeneous deceleration parameter in the absence of modulation.

To go further, we need to calculate $\mathcal{R}_L(\mathbf{x},t)$ and its time derivatives in the late-time accelerating expanding Universe and relate it to its primordial value at the end of inflation $\mathcal{R}_{L\,\rm pri}$. To find the time evolution of curvature perturbations, one can use the dynamical equation of the Bardeen potential Φ. In general, the dynamical equation for the Bardeen potential cannot be solved exactly. Usually, solutions contain elliptic integrals even on the superhorizon scales. Fortunately, for the case at hand, the situations simplify considerably. We consider the late-time universe containing only matter and the cosmological constant. For both of these fluids, the perturbations in pressure is zero. On the other hand, the sound speed of fluctuations is defined in the comoving gauge via $\delta P_c = c_s^2\delta\rho_c$. As a result, for both fluids, the sound speed of fluctuations is zero. Therefore, the effective sound speed of the total perturbations is zero, too. In this limit, one can show that there exists an invariant of the dynamical equation. In addition, one can also show that this invariant quantity coincides with the gauge-invariant curvature perturbation $\mathcal{R}$. To see this, consider the evolution equation for the Bardeen potential [41],

$$u'' - c_s^2\Delta u - \frac{\theta''}{\theta}u = 0, \tag{50}$$

where

$$\theta \equiv \frac{1}{a}\left(1+\frac{\bar{p}}{\bar{\rho}}\right)^{-1/2} \tag{51}$$

and u is defined as $u \equiv \Phi/(\bar{\rho}+\bar{p})^{1/2}$.

As argued above, for our late-time Universe containing only matter and the cosmological constant $c_s = 0$. In this limit, one can easily manipulate the above equation to show that the quantity X defined via

$$X \equiv \theta^2\left(\frac{u}{\theta}\right)' \tag{52}$$

is a constant of integration. On the other hand, using the definitions of u and θ, and noting that $\mathcal{R} = \Phi - H/\dot{H}(\dot{\Phi}+H\Phi)$, one can easily show that $\mathcal{R} \propto X$. As a result, $\mathcal{R}$ is constant too. This indicates that there is no change in the deceleration parameter as given in Eq. (49). This indicates that the long-mode modulation does not induce asymmetry in acceleration expansion associated with the cosmological constant.

Having said this, it is possible to generate dipole asymmetry in late-time acceleration expansion if one

considers other sources of dark energy. Our conclusion above was valid for the cosmological constant in which the sound speed is zero. If one considers dynamical model of dark energy, such as the quintessence model, then the sound speed associated with the scalar field fluctuations is not zero. As a result, in the model containing the mixed fluids of matter and quintessence, $\mathcal{R}$ can be time dependent on superhorizon scales. It is an interesting question to see how the long-mode modulation can generate dipole asymmetry in acceleration expansion for this scenario. However, this is beyond the scope of this work.

Observationally, the possibility of anisotropic acceleration expansion is an intriguing idea. although there are some controversies about the amplitude and the direction of dipole asymmetry in the deceleration parameter; see, e.g., Refs. [42] and [43]. Some older works studied this effect observationally [44]. Also recently, this issue has been revisited by many authors [42,43,45–47]. Bonvin *et al*. showed that the dipole associated with the luminosity distance is a useful observational tool that can be used to determine the Hubble parameter as a function of redshift H(z). They showed that our peculiar velocity relative to the CMB can induce dipole asymmetry on the luminosity distance parameter. There are also some other works dealing with the effects of peculiar velocities associated with the observers and supernovas [48–50]. The typical correction to the luminosity distance parameter due to the peculiar velocities can be estimated to be $\Delta d_L/d_L \simeq v^{\rm pec}/c$ [48,49]. The typical peculiar velocities of supernovas are at the order of $\sim$100 km/s, which leads to $\Delta d_L/d_L \sim 10^{-3}$. One may expect that the dipole correction due to the peculiar velocity of Earth is in the same direction as the dipole of the CMB [51] . But the observed dipole of the luminosity distance is at least 1 order of magnitude lager than the expected asymmetry emerging from peculiar velocities [43]. Moreover, there are also controversies on whether or not its dipole is aligned with the CMB dipole [42]. Recently, Zhao *et al*. claimed that they found a significant anisotropy with dipole amplitude $A_1 = 0.466^{+0.255}_{-0.205}$, which has an angle 95.7° with the CMB dipole [42].

V. CONCLUSION AND DISCUSSIONS

The observed asymmetries in the CMB trigger the interest in long mode modulation as a probable explanation for the observed anomalies. In Ref. [12], it was shown that there is an upper bound consistency relation between the anisotropy of the CMB and the amount of local non-Gaussianity induced by this long-wavelength mode. The CMB temperature anisotropy moments put strict constraints on the amplitude of the anisotropy. In this work, following Ref. [12], we presented a general formalism to investigate the consistency relation between the amplitude of dipole asymmetry and local non-Gaussianity induced by the superhorizon mode. Then, we showed that this long-mode power enhancement introduces a modulation on tensor perturbations. This suggests that further studies check the possibility of the tensor mode perturbation enhancement via the CMB B-mode polarization, which will be studied with more accuracy by the Planck team next year. We have obtained the consistency conditions Eqs. (24) and (25), respectively, in the attractor and nonattractor single-field inflationary models for the ratio $A_T/A_{\mathcal{R}}$. As discussed, the key point is that the tensor modes remain frozen after horizon crossing so any modulation of the long mode on tensor perturbations is encoded at and near the time of horizon crossing. In this view, tensor perturbations are insensitive to features happening at the end or after inflation, such as in the curvaton scenario.

Having said this, none of these two single-field scenarios can produce a detectable A_T. Single-field slow-roll models fail to generate large enough dipole asymmetry in the CMB curvature perturbation power spectrum, so their prediction is $A_T \ll 0.03$. On the other hand, nonattractor models are able to generate large enough dipole asymmetry in the CMB curvature perturbation power spectrum with large enough $f_{\rm NL}^{\rm loc}$ as given in Eq. (18). However, in the nonattractor model, it turns out that ϵ and r are very small, so from the consistency condition Eq. (25), we obtain that A_T is too small to be detectable. Having said this, our consistency condition Eq. (24) should be viewed as a proof of concept that, in principle, a long-mode modulation can yield dipole asymmetry in the tensor perturbations power spectrum. In practice, one has to look for a multiple-field model of inflation to see if a large observable A_T can be generated.

Recently, in Ref. [52], the Maldacena consistency condition that $f_{\rm NL} \sim 1 - n_s$ has been revisited. It is argued that for the standard single-field slow-roll models, considering all contributions, one finds $f_{\rm NL} = 0$ with corrections quadratic in k_L. Having said this, our results, as long as observational considerations are concerned, are intact. This is because, in order to have observable dipole asymmetry, one has to go beyond the simple single-field slow-roll inflation models [12], such as nonattractor models, in which the argument of Ref. [52] does not apply.

As another interesting example, we have looked into effects of long-mode modulation on the halo bias parameter. Defining the bias dipole asymmetry parameter, A_b, we found an upper bound on A_b given by Eqs. (39) and (42). We found that $A_b \propto \nabla(\nabla^2\mathcal{R}_L)$. This implies that, in general, the direction of bias dipole is different than the direction of the CMB power spectrum dipole. Furthermore, the amplitude of the bias dipole compared to the amplitude of the CMB power spectrum is suppressed by the factor $f_{\rm NL}(x_{\rm LSS}/x_{\rm CMB})$. As a result, to get a higher value of A_b, one has to look at higher redshift structures that have a higher value of $x_{\rm LSSS}/x_{\rm CMB}$. We argued that an $\mathcal{O}(20\%)$ modulation in the bias parameter can be obtained for the matter power spectrum in 21 cm observations with $z \sim 10$.

However, in general, the detection of anisotropy in the bias parameter is more difficult than the anisotropy in distances. This is because we need enough statistics (i.e., number of galaxies) in different directions in order to reduce the shot noise in the galaxy power spectrum and investigate the change in the bias parameter.

Finally, we have studied the effects of long-mode modulation on the acceleration expansion. We have shown that in ΛCDM no dipole asymmetry in the acceleration expansion is generated. This is because in a ΛCDM background $\mathcal{R}$ is conserved on superhorizon scales so the effects of $\mathcal{R}$ can be absorbed into a constant coordinate transformation. To induce dipole asymmetry in acceleration, one has to look for models in which dark energy is realized dynamically, i.e., in the quintessence model, in which the sound speed of scalar perturbations is not zero and for the mixture of the matter and the dark energy fluids $\mathcal{R}$ can evolve on superhorizon scales.

In the early Universe cosmological backgrounds, the long-mode modulation can change the Hubble expansion rate and introduce a dipole anisotropy on it. So it is natural to think that cosmological parameters that are related to the Hubble expansion are affected by the long-mode modulations. For example, the observations that use the Baryon Acoustic Oscillations as a standard ruler will be affected because the angular diameter distance and the sound horizon of baryonic oscillations are modulated. The other interesting example is the study of big bang nucleosynthesis (BBN) in the presence of long-mode modulation. As in standard BBN calculations, we have to compare the rate of nuclear interactions with the rate of the Hubble expansion. The former is a property of particle physics and nuclear physics that are not affected by the long mode, while the Hubble expansion rate is affected by the long-mode modulation. As a result, one expects to see dipole asymmetry in hydrogen and helium distributions. It will be an interesting question to study these predictions in details and compare them with the observations.

Our main goal in this work was to demonstrate that if the observed dipole asymmetry in the CMB power spectrum is from the long mode modulation then this effect will also show its fingerprints on different cosmological observables relevant to different cosmological histories. One can find the consistency conditions relating the amplitude of the CMB dipole asymmetry to the dipole asymmetries induced in the power spectrum of tensor perturbations and the halo bias parameter. A detection or otherwise of any of these predicted asymmetries will have profound implications on inflation dynamics and also for the possible preinflationary physics.

ACKNOWLEDGMENTS

We would like to thank Razieh Emami, Hoda Ghodsi, Eiichiro Komatsu, and Sadegh Movahed for useful discussions. We are grateful to Amir Hossein Tajdini for assistances in calculating the scalar-tensor-tensor cross-correlation in the Appendix.

APPENDIX: ANALYSIS OF $\langle \mathcal{R} h_{ij} h_{kl} \rangle$ FOR THE NONATTRACTOR MODEL

In Sec. II B, we have borrowed Maldacena's analysis [23] for the three-point function $\langle \mathcal{R} h_{ij} h_{kl} \rangle$ to obtain the relation between A_T and $A_{\mathcal{R}}$ in the attractor single-field models as given in Eq. (24). Here, we generalize Maldacena's analysis to nonattractor inflation models in which $\mathcal{R}$ is not conserved on superhorizon scales during the nonattractor phase.

We consider the single-field nonattractor models given by the action [53]

$$S = \int d^4x \left[\frac{M_P^2}{2} R + P(X, \phi) \right], \tag{A1}$$

in which $X \equiv -g^{\mu\nu} \partial_\mu \phi \partial_\nu \phi / 2$. The above action is not the most general action for the single-field models, but it is generic enough, which can shed light on the value of $\langle \mathcal{R} h_{ij} h_{kl} \rangle$ in the nonattractor scenarios.

To perform the perturbation analysis, we chose the comoving gauge in which $\delta\phi = 0$ and the tensor perturbations h_{ij} are written as

$$h_{ij} = a^2(t) e^{2\mathcal{R}} \hat{h}_{ij}, \tag{A2}$$

in which $\det \hat{h}_{ij} = 1$. To second order, we have

$$\hat{h}_{ij} \simeq \delta_{ij} + \gamma_{ij} + \frac{1}{2} \gamma_{il} \gamma_{lj}, \tag{A3}$$

in which $\gamma_{ii} = \gamma_{ij,i} = 0$, so the tensor perturbations are transverse and traceless.

We are interested in cubic action containing one scalar perturbation and two gravitons. We skip the details of this analysis and provide the final form of the cubic action,

$$S_{\mathcal{R}\gamma^2} = \int d^4x \frac{\epsilon a^5}{2 c_s^2} \dot{\gamma}_{ij} \dot{\gamma}_{ij} \partial^{-2} \dot{\mathcal{R}}, \tag{A4}$$

supplemented with the field redefinitions

$$\mathcal{R} = \mathcal{R}_c - \frac{1}{32} \gamma_{ij} \gamma_{ij} + \frac{1}{16} \partial^{-2} (\gamma_{ij} \partial^2 \gamma_{ij}) \tag{A5}$$

and

$$\gamma_{ij} = \gamma_{ijc} - \frac{a^2 \epsilon}{c_s^2} (\partial^{-2} \dot{\mathcal{R}}_c) \dot{\gamma}_{ij}. \tag{A6}$$

Here, $\epsilon = -\dot{H}/H^2$ is the slow-roll parameter, and c_s is the sound speed of scalar perturbations.

Compared to attractor cases, there are some important modifications that one has to take into account. First, the wave function of $\mathcal{R}$ is different in the nonattractor model so one has to take this into account in the in-in integrals [53]. Second, on superhorizon scales, $\dot{\mathcal{R}}$ is not negligible, so, in contrast to Maldacena's analysis [23], one cannot neglect the contribution of $\dot{\mathcal{R}}$ in field redefinition, Eq. (A6).

Putting all the contributions together, and skipping the details, we obtain the following result for the correlation function between one scalar and two gravitons in the Fourier space:

$$\langle \mathcal{R}_{\mathbf{k}_1}\gamma^{s_2}_{\mathbf{k}_2}\gamma^{s_3}_{\mathbf{k}_3}\rangle = (2\pi)^3\delta^3\left(\sum \mathbf{k}_i\right)\frac{P_{\mathcal{R}k_1}(t_e)}{k_2^3k_3^3}\epsilon(t_e)H^2\delta_{s_2s_3}\left[-\frac{c_sk_1^3}{2}+\frac{c_s}{2}k_1(k_2^2+k_3^2)+\frac{24c_sk_1}{K^3}k_2^2k_3^2\left(k_2+k_3-\frac{k_2k_3}{K}\right)\right.$$
$$\left.-\frac{8k_2^2k_3^2}{K}-\frac{3k_2^2k_3^2}{c_sk_1K}(k_2-k_3)^2\left(\frac{1}{c_sk_1}+\frac{1}{K}\right)+\frac{9}{K^2}k_2^2k_3^2(k_2+k_3)-\frac{12c_s}{K^2}k_1k_2^2k_3^2\right]. \tag{A7}$$

Here, $K \equiv c_sk_1+k_2+k_3$, s_2 and s_3 are the graviton polarizations, and t_e represents the time of the end of the nonattractor phase. To simplify the analysis, we have assumed that c_s and H are nearly constant during inflation.

The above formula has the interesting property that the momentum associated with the scalar perturbations, k_1, always comes with a factor of c_s. Physically, this make sense because for the scalar perturbations the moment of "sound horizon" is determined by $c_sk_1 = aH$ while for the tensor perturbations with momenta k_2 and k_3, it is the usual horizon crossing, $k_{2,3} = aH$, that matters.

In the squeezed limit in which $k_1 \ll k_1 \simeq k_3$, we get

$$\langle \mathcal{R}_{\mathbf{k}_1}\gamma^{s_2}_{\mathbf{k}_2}\gamma^{s_3}_{\mathbf{k}_3}\rangle = (2\pi)^3\delta^3\left(\sum \mathbf{k}_i\right)\frac{P_{\mathcal{R}k_1}(t_e)}{2k_2^3}\epsilon(t_e)H^2\delta_{s_2s_3}. \tag{A8}$$

Curiously, there are two leading terms proportional to $1/c_s^2$ (in the limit of small c_s), which canceled each other, so Eq. (A8) represents the effects of the remaining subleading term that is independent of the $1/c_s$ factor.

Comparing with the definition of $f_{\rm NL}^{\mathcal{R}h}$, given in Eq. (7), and summing over the two polarizations s_1 and s_2, we obtain

$$\frac{12}{5}f_{\rm NL}^{\mathcal{R}h} = 2\epsilon(t_e). \tag{A9}$$

Noting that $2\epsilon(t_e) = -n_T$, our result for $f_{\rm NL}^{\mathcal{R}h}$ in nonattractor models coincides with the result obtained in Maldacena's analysis for attractor models, given by Eq. (23).

[1] A. H. Guth, Phys. Rev. D **23**, 347 (1981); A. A. Starobinsky, Phys. Lett. **91B**, 99 (1980); K. Sato, Mon. Not. R. Astron. Soc. **195**, 467 (1981); Phys. Lett. **108B**, 103 (1982); A. Albrecht and P. J. Steinhardt, Phys. Rev. Lett. **48**, 1220 (1982).

[2] L. P. Grishchuk and Ia. B. Zeldovich, Astron. Zh. **55**, 209 (1978); Sov. Astron. **22**, 125 (1978).

[3] P. A. R. Ade *et al.* (Planck Collaboration), arXiv:1303.5083.

[4] H. K. Eriksen, F. K. Hansen, A. J. Banday, K. M. Gorski, and P. B. Lilje, Astrophys. J. **605**, 14 (2004); **609**, 1198(E) (2004); H. K. Eriksen, A. J. Banday, K. M. Gorski, F. K. Hansen, and P. B. Lilje, Astrophys. J. **660**, L81 (2007).

[5] L. Dai, D. Jeong, M. Kamionkowski, and J. Chluba, Phys. Rev. D **87**, 123005 (2013).

[6] A. R. Pullen and M. Kamionkowski, Phys. Rev. D **76**, 103529 (2007).

[7] A. L. Erickcek, M. Kamionkowski, and S. M. Carroll, Phys. Rev. D **78**, 123520 (2008).

[8] C. Gordon, Astrophys. J. **656**, 636 (2007).

[9] A. L. Erickcek, S. M. Carroll, and M. Kamionkowski, Phys. Rev. D **78**, 083012 (2008).

[10] A. R. Liddle and M. Corts, Phys. Rev. Lett. **111**, 111302 (2013).

[11] D. H. Lyth, J. Cosmol. Astropart. Phys. 12 (2007) 016.

[12] M. H. Namjoo, S. Baghram, and H. Firouzjahi, Phys. Rev. D **88**, 083527 (2013).

[13] D. H. Lyth, arXiv:1304.1270; J. F. Donoghue, K. Dutta, and A. Ross, Phys. Rev. D **80**, 023526 (2009).

[14] L. Wang and A. Mazumdar, Phys. Rev. D **88**, 023512 (2013).

[15] A. L. Erickcek, C. M. Hirata, and M. Kamionkowski, Phys. Rev. D **80**, 083507 (2009).

[16] J. McDonald, J. Cosmol. Astropart. Phys. 07 (2013) 043.

[17] A. Mazumdar and L. Wang, J. Cosmol. Astropart. Phys. 10 (2013) 049.

[18] Z.-G. Liu, Z.-K. Guo, and Y.-S. Piao, Phys. Rev. D **88**, 063539 (2013).

[19] F. Schmidt and L. Hui, Phys. Rev. Lett. **110**, 011301 (2013); Publisher note **110**, 059902 (2013).
[20] S. Prunet, J.-P. Uzan, F. Bernardeau, and T. Brunier, Phys. Rev. D **71**, 083508 (2005).
[21] C. T. Byrnes, S. Nurmi, G. Tasinato, and D. Wands, J. Cosmol. Astropart. Phys. 03 (2012) 012.
[22] S. Kanno, M. Sasaki, and T. Tanaka, Prog. Theor. Exp. Phys. **2013**, 111E01 (2013).
[23] J. M. Maldacena, J. High Energy Phys. 05 (2003) 013.
[24] M. H. Namjoo, H. Firouzjahi, and M. Sasaki, Europhys. Lett. **101**, 39001 (2013).
[25] X. Chen, H. Firouzjahi, M. H. Namjoo, and M. Sasaki, Europhys. Lett. **102**, 59001 (2013).
[26] Q.-G. Huang and Y. Wang, J. Cosmol. Astropart. Phys. 06 (2013) 035.
[27] X. Chen, H. Firouzjahi, M. H. Namjoo, and M. Sasaki, J. Cosmol. Astropart. Phys. 09 (2013) 012.
[28] P. A. R. Ade *et al.* (Planck Collaboration), arXiv:1303.5084.
[29] C. M. Hirata, J. Cosmol. Astropart. Phys. 09 (2009) 011.
[30] W. J. Percival *et al.*, Astrophys. J. **657**, 645 (2007).
[31] H. J. Mo and S. D. M. White, Mon. Not. R. Astron. Soc. **282**, 347 (1996).
[32] J. E. Gunn and J. R. Gott III, Astrophys. J. **176**, 1 (1972).
[33] S. Baghram, M. H. Namjoo, and H. Firouzjahi, J. Cosmol. Astropart. Phys. 08 (2013) 048.
[34] J. M. Bardeen, J. R. Bond, N. Kaiser, and A. S. Szalay, Astrophys. J. **304**, 15 (1986).
[35] W. H. Press and P. Schechter, Astrophys. J. **187**, 425 (1974).
[36] L. Anderson *et al.*, Mon. Not. R. Astron. Soc. **427**, 3435 (2013).
[37] H. Zhan, J. Cosmol. Astropart. Phys. 08 (2006) 008.
[38] E. W. Kolb, S. Matarrese, A. Notari, and A. Riotto, arXiv: hep-th/0503117.
[39] G. Geshnizjani, D. J. H. Chung, and N. Afshordi, Phys. Rev. D **72**, 023517 (2005).
[40] C. M. Hirata and U. Seljak, Phys. Rev. D **72**, 083501 (2005).
[41] V. Mukhanov, *Physical Foundations of Cosmology* (Cambridge University Press, Cambridge, England, 2005).
[42] W. Zhao, P. X. Wu, and Y. Zhang, Int. J. Mod. Phys. D **22**, 1350060 (2013).
[43] R.-G. Cai, Y.-Z. Ma, B. Tang, and Z.-L. Tuo, Phys. Rev. D **87**, 123522 (2013).
[44] D. J. Schwarz and B. Weinhorst, Astron. Astrophys. **474**, 717 (2007).
[45] S. A. Appleby and E. V. Linder, Phys. Rev. D **87**, 023532 (2013).
[46] B. Kalus, D. J. Schwarz, M. Seikel, and A. Wiegand, Astron. Astrophys. **553**, A56 (2013).
[47] L. Campanelli, P. Cea, G. L. Fogli, and A. Marrone, Phys. Rev. D **83**, 103503 (2011).
[48] T. M. Davis *et al.*, Astrophys. J. **741**, 67 (2011).
[49] L. Hui and P. B. Greene, Phys. Rev. D **73**, 123526 (2006).
[50] J. Colin, R. Mohayaee, S. Sarkar, and A. Shafieloo, Mon. Not. R. Astron. Soc. **414**, 264 (2011).
[51] C. Bonvin, R. Durrer, and M. Kunz, Phys. Rev. Lett. **96**, 191302 (2006).
[52] E. Pajer, F. Schmidt, and M. Zaldarriaga, Phys. Rev. D **88**, 083502 (2013).
[53] X. Chen, H. Firouzjahi, E. Komatsu, M. H. Namjoo, and M. Sasaki, J. Cosmol. Astropart. Phys. 12 (2013) 039.